TEXTURE ANALYSIS BY (110) POLE FIGURE FOR A SPD PROCESSED Ti-25Ta-25Nb ALLOY

Vasile Dănuț COJOCARU[1], Doina RĂDUCANU[2],
Ion CINCA[3], Andreea CĂPRĂRESCU[4]

A fost investigată textura obținută prin Deformare Plastică Severă în aliajul Ti-25Ta-25Nb cu ajutorul difracției de raze X. În urma investigațiilor s-a observat că principala componentă texturală dezvoltată o constituie textura de laminare $\{001\} < 110 >$*, cu orientări specifice cuprinse între* $\{001\} < 1\bar{1}0 >$ *şi* $\{001\} < \bar{1}\bar{1}0 >$*. De asemenea, au fost identificate şi fibrele texturale γ şi α. Pentru fibrajul γ s-au observat orientări specifice cuprinse între* $\{111\} < 1\bar{1}0 >$ *şi* $\{111\} < \bar{1}\bar{1}2 >$*; în timp ce pentru fibrajul α s-au observat orientări specifice cuprinse între* $\{001\} < 1\bar{1}0 >$ *şi* $\{112\} < \bar{1}\bar{1}2 >$*.*

Texture of Severe Plastic Deformation (SPD) processed Ti-25Ta-25Nb alloy was investigated by X-ray diffraction. A strong $\{001\} < 110 >$ *rolling texture, with main orientation component spreads from* $\{001\} < 1\bar{1}0 >$ *to* $\{001\} < \bar{1}\bar{1}0 >$*, was obtained. High intensity texture fibres (γ-fibre and α-fibre) were obtained also. In the case of γ-fibre the main orientation component spreads from* $\{111\} < 1\bar{1}0 >$ *to* $\{111\} < \bar{1}\bar{1}2 >$*; while in the case of α-fibre the main orientation component spreads from* $\{001\} < 1\bar{1}0 >$ *to* $\{112\} < \bar{1}\bar{1}2 >$*.*

Keywords: β titanium alloys; texture, pole figure

1. Introduction

During the last decade β-type Titanium alloys composed of non-toxic elements have attracted attention as biomedical and/or superelastic material [1,2] due to their excellent biocompatibility with no adverse cytotoxicity, excellent corrosion resistance and a good combination of mechanical properties such as high strength and low elastic modulus [3,4].

[1] Reader, Materials Science and Engineering Faculty, University POLITEHNICA of Bucharest, Romania; PostDoc fellow, National Institute for Research and Development in Microtechnologies, Romania, e-mail: dan.cojocaru@mdef.pub.ro,
[2] Prof., Materials Science and Engineering Faculty, University POLITEHNICA of Bucharest, Romania
[3] Reader, Materials Science and Engineering Faculty, University POLITEHNICA of Bucharest, Romania
[4] PhD student, Materials Science and Engineering Faculty, University POLITEHNICA of Bucharest, Romania

Typically the β-type Titanium alloys are prepared by casting followed by hot/cold working and heat treatment. The texture developed during the thermo-mechanical process affects the alloys behaviour, being very important to carry out texture studies in order to obtain the maximum level of properties [1].

Polycrystalline materials contain many millions of grains. Each grain in a specimen has a different crystallographic orientation from its neighbours. When the orientation of grains is not random, the materials are textured. Otherwise, the material is not textured. In order to describe texture one must determine how grains in a polycrystalline specimen are oriented in respect to the sample reference frame [5-7].

There are several experimental methods that can be used to measure texture. The most popular one is X-ray diffraction. The result of texture measurement obtained using the X-ray diffraction method, is represented by a pole figure, which is a stereographic projection of pole density as a function of pole orientation. The pole figure is the starting point of X-ray texture analysis [5-7].

The aim of this research is to investigate the developed texture in the Severe Plastic Deformation (SPD) processed Ti-25Ta-25Nb alloy (β-type Titanium alloy), to identify the main texture modes and potentially developed texture fibres.

2. Methods

2.1. Alloy synthesis

The investigated alloy has been produced using a vacuum induction melting in levitation furnace FIVE CELES with nominal power 25 kW and melting capacity 30 cm^3, starting from elemental components. The obtained chemical composition in wt.% was: 70%Ti; 25%Ta; 25%Nb.

2.2. Severe Plastic Deformation (SPD) of the Ti-25Ta-25Nb alloy

The as-cast alloy was processed by Severe Plastic Deformation (SPD) procedure, as is shown in Fig. 1. The SPD procedure consists in a first cold-rolling deformation up to 85.83% deformation degree, followed by a recrystallization heat treatment at 850°C for 30 minutes, in argon protective atmosphere. The recrystallization heat treatment was performed in order to remove the effects of strain-hardening. For the recrystallization heat treatment a GERO SR 100x500 heat treatment oven has been used.

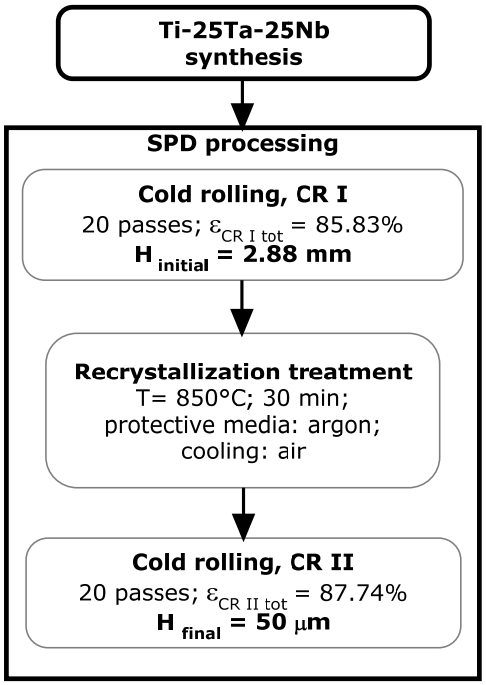

Fig. 1. SPD processing route.

After recrystallization, a second cold-rolling deformation was performed, up to 87.74% deformation degree, in order to obtain the final sheet thickness of about 50 μm. All cold-rollings were performed using a Mario di Maio LQR120AS rolling-mill. The rolling speed was 3 m/min.

2.3. XRD experiments

SPD processed specimens were XRD characterized using a PANalytical X'Pert PRO MRD diffractometer, with a wavelenght of Cu k-alpha (λ = 1.5418 A). Pole figure (110) was obtained. Pole figure raw data was fitted and analysed using MTEX v3.2.2 open source software package [8,9].

3. Results and discussion

Fig. 2 shows collected raw data for (110) pole figure, in the case of 2D (Fig. 2.a) and 3D representation (Fig. 2.b). The (110) pole figure was plotted in respect to the following directions (sample reference frame): [100] – rolling direction (RD); [010] – transversal direction (TD) and [001] – normal direction (ND).

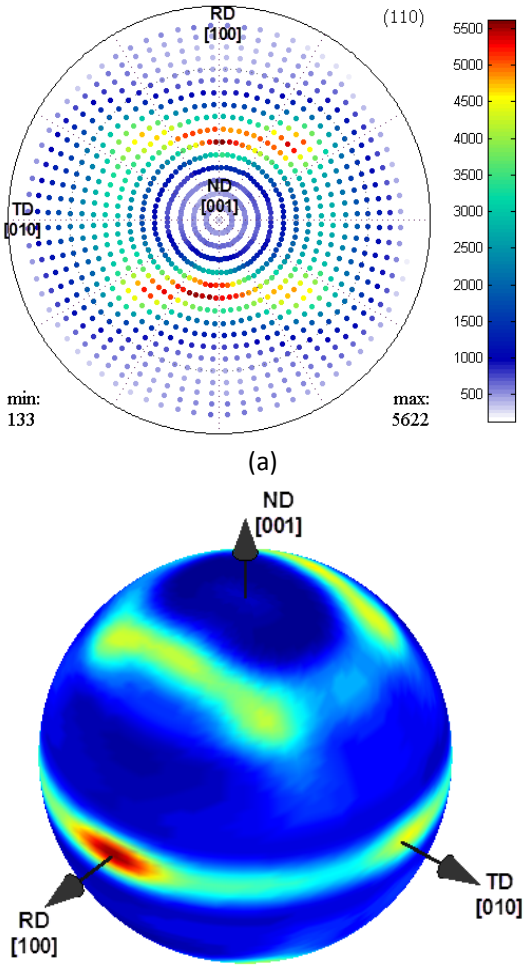

Fig. 2. Representation of raw data (110) pole figure for SPD processed Ti-25Ta-25Nb alloy: a- 2D representation; b- 3D representation.

The (110) pole figure, see Fig. 2a and 2.b, shows intensity distributions characteristic for bcc (Body Centred Cubic) crystalline structures.

A well-developed rolling-texture is confirmed in as-rolled specimen as shown in Fig. 2. The (110) pole figure shows four peaks symmetrically located around 45° from the centre. The four peaks are located at 45° from both RD and TD. This means that the rolling direction is parallel to [110] crystal directions.

While the pole figure shows how the specified crystallographic direction of grains are distributed in the sample reference frame, the inverse pole figure shows how the selected direction in the sample reference frame is distributed in

the reference frame of the crystal. Fig. 3 shows the (110) inverse pole figure for RD, TD and ND directions.

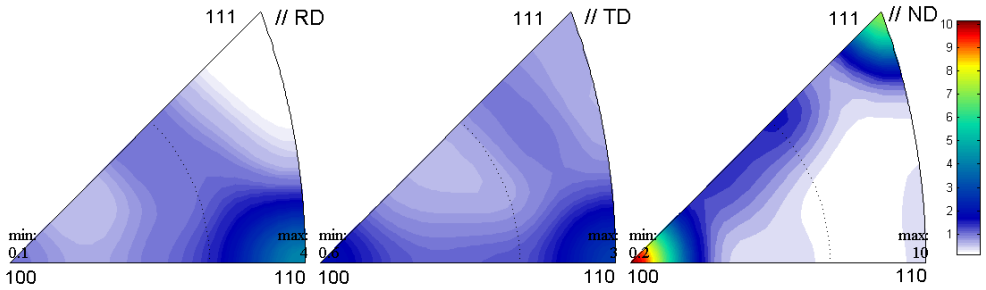

Fig. 3. Representation of (110) Inverse Pole Figure:
a- for RD [100] direction; b- TD [010] direction; c- ND [001] direction.

For example, if we consider the RD direction, the inverse pole figure shows us which crystallographic directions in the polycrystalline material are most likely parallel to the sample rolling direction (see Fig. 3.a). In this case one can see that the [110]//RD pair reaches an intensity close to 4. In the case of TD direction, one can see that two low intensity pairs can be formed: [100]//TD and respectively [110]//TD, with both intensities close to 2 (see Fig. 3.b). The highest intensities are obtained in the case of [100]//ND and [111]//ND pairs, in this case the intensities reach values close to 10 respectively 6 (see Fig. 3.c). In this way most likely the developed texture during Severe Plastic Deformation (SPD) processing will show [100]//ND, [111]//ND and [110]//RD components.

Since the properties of many important engineering materials are strongly direction-dependent, the inverse pole figure is very useful in predicting and calculating the average properties of polycrystalline material along a chosen direction [10,11].

Using raw pole figure data the Orientation Distribution Function was calculated and plotted. In order to calculate the ODF, few assumptions were made: the crystalline symmetry was indexed in cubic m-3m system and the specimen symmetry in triclinic -I system. The rotation angle (φ_2) used to represent the ODF's was 90°, divided in 6 sections (15° steps).

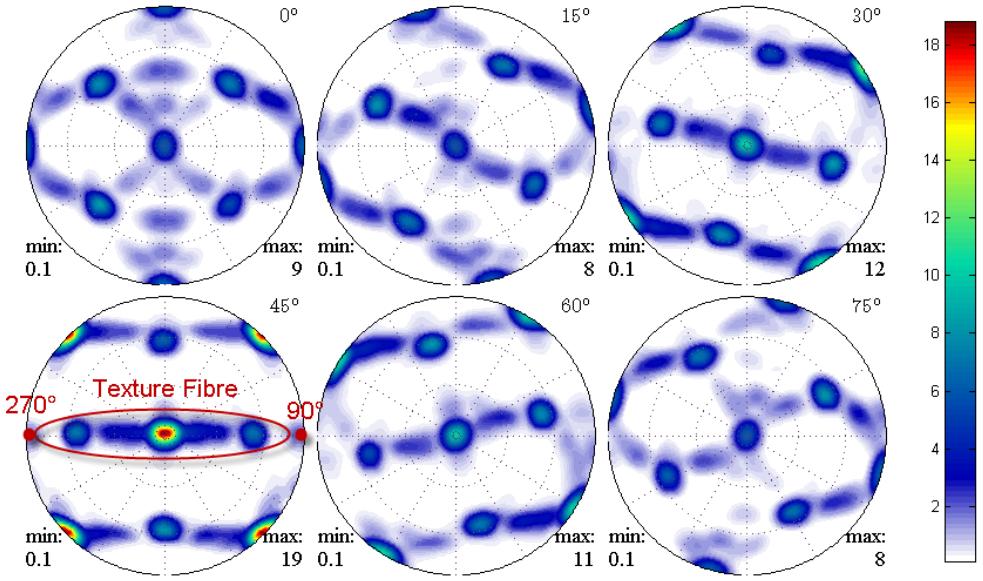

Fig. 4. Calculated Orientation Distribution Function (ODF) for (110) pole figure.

The crystallographic textures are typically presented in the reduced Euler space (φ_1 = (0° – 360°); Φ_2 = (0° – 90°); φ_2 = (0° – 90°)). The most relevant texture fibres for bcc metals are [12-14]:

- α-fibre (crystallographic fibre axis <110> parallel to the rolling direction, including major components: {001}<110>; {112}<110>;{111}<110>);
- γ-fibre (crystallographic fibre axis <111> parallel to the normal direction, including major components: {110}<110>; {111}<112>);
- η-fibre (crystallographic fibre axis <001> parallel to the rolling direction, including major components: {001}<100>; {011}<100>);
- ζ-fibre (crystallographic fibre axis <011> parallel to the normal direction, including major components: {011}<100>; {011}<211>; {011}<111>); {011}<011>);
- ε-fibre (crystallographic fibre axis <011> parallel to the transversal direction, including major components: {001}<011>; {112}<111>; {111}<112>); {011}<100>);
- θ-fibre (crystallographic fibre axis <001> parallel to the normal direction, including major components: {001}<100>; {001}<110>).

In the case of ODF of the (110) pole figure, a high intensity central peak is observed. Other four less intense peaks, located at 45° from the centre and 45° from both RD and TD are observed too (see Fig. 4), the ODF shows a maximum orientation density, of about 18, for rotation angle (φ_2) equal to 45°. A fibre

texture is observed also for rotation angle (φ_2) equal to 45°, this fibre being developed along 90° – 270° rotation angle (φ_1).

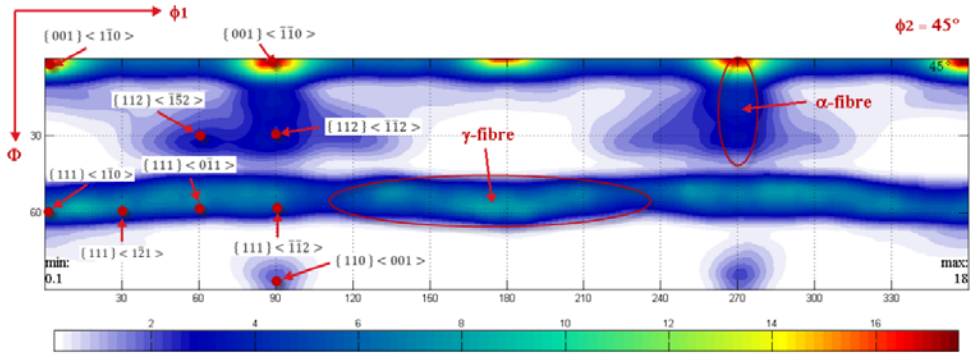

Fig. 5. The φ_2 = 45° section of the Orientation Distribution Function (ODF).

Fig. 5 shows the φ_2 = 45° section of the ODF, were can be observed that few texture modes are present:

- high intensity texture modes $\{001\}<1\bar{1}0>$ and $\{001\}<\bar{1}\bar{1}0>$: which shows a maximum orientation density close to 18; Both $\{001\}<1\bar{1}0>$ and $\{001\}<\bar{1}\bar{1}0>$ modes belonging to θ-fibre ({001}<110> family) and being caused by grains shear during SPD processing;
- well-developed α and γ–fibres; The main component of α–fibre spreads from $\{001\}<1\bar{1}0>$ to $\{112\}<\bar{1}\bar{1}2>$ and the γ–fibre from $\{111\}<1\bar{1}0>$ to $\{111\}<\bar{1}\bar{1}2>$. The orientation density of α–fibre reaches a value close to 5 while the γ–fibre shows a double orientation density, close to 10, showing that the γ–fibre being the most important developed fibre during SPD processing;
- low intensity texture modes $\{110\}<001>$ and $\{112\}<\bar{1}\bar{5}2>$: showing orientation density close to 2 and respectively 4.

During the plastic deformation of the alloy, grain orientation changes take place as a consequence of shear on specific favourable oriented crystal planes and directions. In the case of materials with bcc structure, slip can occur on {110}<111>,{112}<111> and {113}<111> slip systems. Imposed strain and constraint between neighbouring grains affect the choice and number of slip systems. Slip activation and their variation within and between grains determine the deformation microstructure and the change of grain orientation.

During cold-rolling, dislocation glide will force the slip planes to rotate towards the tensile axis due to the constraint of the axis, and the rotation axis is [hkl]x[uvw], where [hkl] is the normal of the slip plane and the [uvw] is the slip

direction, being possible to activate different texture modes {hkl}<uvw> by a mechanism of formation and rotation of microbands [15].

The development of $\{001\}<110>$ texture is characteristic of the bcc materials in the presence of share [16,17]. The γ–fibre ({110}<110> and {111}<112> modes) is well-developed in bcc materials under high loads, due to the plain strain deformation state during deformation [16,17]. The $\{001\}<110>$ texture is a major rolling texture component observed in bcc metals such as α-Fe, Ta, Mo, β-Ti and W [18-20].

It was reported that a correlation between the deformation microstructure and the crystal orientation can be developed; it was suggested that during cold-rolled deformation, the α-fibre grains can use as many as seven independent slip systems, which allow homogeneous deformation in α-fibre grains. It was also indicated that the dislocation structures is constantly evolving during cold deformation [15].

In the case of SPD processed Ti-25Ta-25Nb alloy one can say that the developed texture mainly shows high intensity share texture modes and well-developed α and γ–fibres, most well-developed fibre being the γ–fibre (showing a double intensity of orientation density as compared with α–fibre). Also, the share texture modes show almost double intensity of orientation densities as compared with fibre modes.

4. Conclusions

The texture of SPD processed Ti-25Ta-25Nb alloy is characterized by the presence of:

- strong rolling texture $\{001\}<110>$; main orientation component spreads from $\{001\}<1\bar{1}0>$ to $\{001\}<\bar{1}\bar{1}0>$; showing an orientation density close to 18;
- well-developed γ-fibre; main orientation component spreads from $\{111\}<1\bar{1}0>$ to $\{111\}<\bar{1}\bar{1}2>$; showing an orientation density close to 10;
- well-developed α-fibre; main orientation component spreads from $\{001\}<1\bar{1}0>$ to $\{112\}<\bar{1}\bar{1}2>$; showing an orientation density close to 5.

Acknowledgement

This paper was supported by the project "Human Resource Development by Postdoctoral Research on Micro and Nanotechnologies", Contract

POSDRU/89/1.5 /S/63700, project co-funded from European Social Fund through Sectorial Operational Program Human Resources 2007-2013.

R E F E R E N C E S

[1] *H.Y. Kim, T. Sasaki, K. Okutsu, J.I. Kim, T. Inamura, H. Hosada and S. Myazaki*, "Texture and shape memory behaviour of Ti-22Nb-6Ta alloy", in Acta Materialia, **vol. 24**, 2006, pp. 423-433.

[2] *H. Hosoda, Y. Fukui, T. Inamura, K. Wakashima, S. Miyazaki and K. Inoue*, "Mechanical Properties of Ti-Base Shape Memory Alloys", in Materials Science Forum, **vol. 426-432**, 2003, pp. 3121-3126.

[3] *M. Tane, A. Akita, T. Nakano, K. Hagihara, Y. Umakoshi, M. Niinomi and H. Nakajima*, "Peculiar elastic behavior of Ti–Nb–Ta–Zr single crystals", in Acta Materialia **vol. 56**, 2008, pp. 2856-2863.

[4] *P. John S. Buenconsejo, H.Y. Kim and S. Miyazaki*, "Effect of ternary alloying elements on the shape memory behavior of Ti–Ta alloys", in Acta Materialia **vol. 57**, 2009, pp. 2509-2515

[5] *H. J. Bunge*, Texture analysis in materials science: mathematical methods, Butterworths, London, 1982.

[6] U.*F. Kocks, C.N. Tomé, H.R. Wenk*, Texture and anisotropy: preferred orientations in polycrystals and their effect on materials properties, Cambridge University Press, Cambridge, 2000.

[7] *F. Larson*, Properties of Textured Titanium Alloys, Metals and Ceramics Information Center, Columbus, USA, 1974.

[8] *F. Bachmann, R. Hielscher and H. Schaeben*, "Texture Analysis with MTEX - Free and Open Source Software Toolbox", in Solid State Phenomena **vol. 160**, 2010, pp. 63-68.

[9] *F. Bachmann, R. Hielscher, P. E. Jupp, W. Pantleon, H. Schaeben and E. Wegert*, "Inferential statistics of electron backscatter diffraction data from within individual crystalline grains", in Journal of Applied Crystalography, **vol. 43**, 2010, pp. 1338-1355.

[10] *N.P. Gurao and S. Suwas*, "Study of texture evolution in metastable β-Ti alloy as a function of strain path and its effect on α transformation texture", in Materials Science and Engineering A, **vol. 504**, 2009, pp. 24-35.

[11] *Z. Ahmed and A. ul Haq*, "Texture, microstructure and magnetic properties of Fe-28Cr-15Co-3.5Mo permanent magnet", in Journal of Magnetism and Magnetic Materials, **vol. 321**, 2009, pp. 325-329.

[12] *M. Holscher, D. Raabe and K. Lucke*, "Relationship between rolling textures and shear textures in f.c.c. and b.c.c. metals", in Acta Metallurgica et Materialia, **vol. 42**, 1994, pp. 879-886.

[13] *D. Raabe and K. Lucke*, "Textures of ferritic stainless steels", in Materials Science and Technology, **vol. 9**, 1993, pp. 302-312.

[14] *B. Sander and D. Raabe*, "Texture inhomogeneity ina a Ti-Nb based β-titanium alloy after worm rolling and recrystallization", in Materials Science and Engineering A, **vol. 479**, 2008, pp. 236-247.

[15] *C. Chen, M.P. Wang, S. Wang, Y.L. Jia, R.S. Lei, F.X. Zia, B. Huo and H.C. Yu*, "The evolution of cold-rolled deformation microstructure of {001}<110> grains in Ta-7.5wt%W alloys foils", in Journal of Alloys and Compounds, **vol. 513**, 2012, pp. 208-212.

[16] *O. Engler, M.Y. Huh and C.N. Tome*, "A study of through-thickness texture gradient in rolled sheets", in Metallurgical and Materials Transactions A, **vol. 31**, 2000, pp. 2299-2315.

[17] *G. Liu and B.J. Duggan*, "Deformation banding and ferrite-type rolling texture", in Metallurgical and Materials Transactions A, **vol. 32**, 2001, pp. 125-134.
[18] *T. Karthikeyan, A. Dasgupta, R. Khatirkar, S. Saroja, I. Samajdar and M. Vijayalakshmi*, "Effect of cooling rate on transformation texture and variant selection during α→β transformation in Ti–5Ta–1.8Nb alloy", in Materials Science and Engineering A, **vol. 528**, 2010, pp. 549-558.
[19] *S. Banumathy, R.K. Mandal and A.K. Singh*, "Texture and anisotropy of a hot rolled Ti–16Nb alloy", in Journal of Alloys and Compounds, **vol. 500**, 2010, pp. L26-L30.
[20] *Y.B. Park, D.N. Lee and G. Gottstein*, "The evolution of recrystallization textures in body centred cubic metals", in Acta Materialia, **vol. 46**, 1998, pp. 3371-3379.